Motion of a spherical capsule in simple shear flow: influence of the bending resistance

Claire Dupont, Anne-Virginie Salsac, Dominique Barthes-Biesel, Marina Vidrascu, Patrick Le Tallec

CSMA 2013
11e Colloque National en Calcul des Structures
13-17 Mai 2013

Motion of a spherical capsule in simple shear flow: influence of the bending resistance.

Claire Dupont[1,2], Anne-Virginie Salsac[2], Dominique Barthès-Biesel[2], Marina Vidrascu[3], Patrick Le Tallec [1]

[1] Laboratoire de Mécanique des Solides (UMR CNRS 7649), Ecole Polytechnique, email: (dupont, letallec)@lms.polytechnique.fr
[2] Laboratoire de Biomécanique et Bioingénierie (UMR CNRS 7338), Université de Technologie de Compiègne, email: (a.salsac, dbb)@utc.fr
[3] Equipe-projet REO, INRIA Rocquencourt - LJLL UMR 7958 UPMC, email: marina.vidrascu@inria.fr

Résumé — We simulate the motion of an initially spherical capsule in a simple shear flow in order to determine the influence of the bending resistance on wrinkle formation on the membrane. We use a numerical method coupling a nonlinear shell finite element method for the capsule wall mechanics with a boundary integral method to solve the Stokes equation. The capsule wall is discretized with MITC linear triangular shell finite elements. We find that, at low flow strength, buckling occurs in the central region of the capsule. The number of wrinkles on the membrane decreases with the bending stiffness and above a critical value, wrinkles no longer form. For thickness to radius ratios below 5%, the bending stiffness does not have any significant effect on the overall capsule motion and deformation. The mean capsule shape is identical whether the wall is modeled as a shell or a two-dimensional membrane, which shows that the dynamics of thin capsules is mainly governed by shear elasticity and membrane effects.
Mots clés — fluid-structure interaction, shell element, finite element method, boundary integral method

1 Introduction

Bioartificial capsules consisting of an internal liquid droplet enclosed by a thin hyperelastic wall have numerous applications in bioengineering and pharmaceutics, where they are used as vectors for drug targeting or the development of artificial organs. Numerical models are necessary to predict their behavior in an external flow, in particular whether the membrane will rupture or not. When subjected to an external flow, they undergo large deformations and, in some cases, buckling because of the strong fluid-structure viscous coupling with the internal and suspending fluids.

Different numerical methods have been considered to simulate the dynamics of a capsule in an external flow. Many studies have used a fluid solver based on the boundary integral method to solve the Stokes flow equations [6, 7, 4, 9]. Since the velocity field at any position within the fluid domain is given by surface integrals calculated on the geometric boundaries, the method allows to reduce the dimension of the problem by one and to avoid re-meshing the fluid domain at each time step. So far, the capsule wall is typically considered to be infinitely thin with negligible bending stiffness and modeled as a 2D hyperelastic material. The wall equilibrium equation can be written locally at each point (strong form) [6, 7, 4] or in its weak form. In this case, the equation of the force equilibrium on the wall is globally integrated over the capsule surface using a finite element method. A method coupling the boundary integral method with the finite element method was proposed by [9]. This method has the advantage of using the same discretization for the fluids and capsule wall, which allows a Lagrangian tracking of the membrane position with high accuracy. It has been shown to be stable in the presence of in-plane compression. It has thus been possible to study little explored cases, such as the dynamics of a capsule in a pore with a square cross-section [10] or the motion of an ellipsoidal capsule in a simple shear flow, when its revolution axis is initially placed off the shear plane [3].

The present objective is to study the influence of bending resistance on the motion and deformation of a spherical capsule in an external shear flow. The finite elements need to be enriched to take into account the bending stiffness of the capsule wall. We use a MITC (mixed interpolation of the tensorial component) nonlinear shell finite element method that accounts for both membrane and bending effects

[2]. The problem and the numerical method are briefly outlined in §2. We assess the non-linear behavior of the shell finite elements simulating the inflation of a capsule under an internal pressure in §3. The fluid-structure interaction method is validated on the classical test of an initially spherical capsule in simple shear flow in §4. We then investigate the influence of the bending resistance on the capsule motion and on the wrinkle formation.

2 Problem statement

We consider an initially spherical microcapsule (radius ℓ) consisting of a liquid droplet enclosed by a thin membrane. The membrane is a three-dimensional material of thickness η, shear modulus G, Poisson coefficient ν and bending modulus κ. It is modeled as a midsurface shell defined by material properties :

$$G_s = \eta G, \qquad \nu_s = \nu \tag{1}$$

where G_s is the surface shear modulus and ν_s the surface Poisson coefficient.

The capsule is suspended in a simple shear flow in the $(\underline{e}_1, \underline{e}_2)$ plane :

$$\underline{v}^{\infty} = \dot{\gamma} x_2 \underline{e}_1, \tag{2}$$

where $\dot{\gamma}$ is the shear rate. The inner and outer fluids are supposed to be Newtonian and to have the same viscosity μ and density ρ.

Owing to the small capsule size, the inner and outer flow Reynolds numbers $Re = \rho \ell^2 \dot{\gamma}/\mu$ are infinitely small. The dynamics of the microcapsule is mostly governed by the capillary and bending numbers

$$Ca = \frac{\mu \dot{\gamma} \ell}{G_s} \qquad B = \frac{1}{\ell}\sqrt{\frac{\kappa}{G_s}}. \tag{3}$$

The capillary number compares the viscous to the shear forces and the bending number the bending to the shear elastic forces. The latter can also be considererd as the ratio of the membrane thickness η to the sphere radius ℓ.

2.1 Membrane mechanics

The three-dimensional fluid-structure interactions are solved with the model developed by Walter *et al.* [9], which couples a membrane finite element method for the capsule wall deformation with a boundary integral method for the internal and external flows. But contrary to Walter *et al.* [9], we treat the capsule wall as a shell made of an isotropic material. In this subsection, we briefly describe the shell kinematics based on [2] and [8] as well as the mechanical problem solved. The surface tensor components will be designed with Greek indices and the 3D tensor components with Latin indices. We adopt the Einstein summation convention on repeated indices.

The capsule wall is represented as a shell of midsurface $\mathcal{S}$ and thickness η. At each instant of time, the midsurface is defined by the 2D chart $\underline{\phi}(\xi^1, \xi^2)$, which takes values in the bounded open subset $\omega \in \mathbb{R}^2$. It is convenient to define the local covariant base $(\underline{a}_1, \underline{a}_2, \underline{a}_3)$ following the midsurface deformation. The two base vectors $(\underline{a}_1, \underline{a}_2)$ are tangent to the midsurface

$$\underline{a}_\alpha = \underline{\phi}_{,\alpha}, \qquad \alpha = 1,2 \tag{4}$$

where the notation $\cdot_{,\alpha}$ denotes the partial derivative with respect to ξ^α. The third vector $\underline{a}_3$ is the unit normal vector $\underline{n}$ of the capsule midsurface $\mathcal{S}$. The contravariant base $(\underline{a}^1, \underline{a}^2, \underline{a}^3)$ is defined by $a^\alpha \cdot a_\beta = \delta^\alpha_\beta$, with δ^α_β the Kronecker tensor and $\underline{a}^3 = \underline{a}_3 = \underline{n}$.

The three-dimensional position within the capsule wall is given by

$$\underline{\phi}^{3D}(\xi^1, \xi^2, \xi^3) = \underline{\phi}(\xi^1, \xi^2) + \xi^3 \underline{a}_3(\xi^1, \xi^2), \tag{5}$$

for (ξ^1,ξ^2,ξ^3) in the reference domain

$$\omega^{3D} = \left\{ (\xi^1,\xi^2,\xi^3) \in \mathbb{R}^3 / (\xi^1,\xi^2) \in \omega, \xi^3 \in \left] -\frac{\eta(\xi^1,\xi^2)}{2}, \frac{\eta(\xi^1,\xi^2)}{2} \right[\right\}. \tag{6}$$

We define the 3D covariant base vector $(\underline{g}_1,\underline{g}_2,\underline{g}_3)$ such that

$$\underline{g}_\alpha = \underline{\phi}^{3D}_{,\alpha} = \underline{a}_\alpha + \xi^3 \underline{a}_{,\alpha} \qquad \text{and} \qquad \underline{g}_3 = \underline{a}_3. \tag{7}$$

The 3D contravariant base $(\underline{g}^1,\underline{g}^2,\underline{g}^3)$ is likewise defined by $g^m \cdot g_n = \delta^m_n$. The components of the 3D metrics tensor are

$$g_{\alpha\beta} = \underline{g}_\alpha \cdot \underline{g}_\beta, \qquad g_{\alpha 3} = 0, \qquad g_{33} = 1. \tag{8}$$

We assume that the displacement satisfies the Reissner-Mindlin kinematical assumption, i.e. the material line orthogonal to the midsurface remains straight and unstretched during deformation. The displacement is then expressed by

$$\underline{u}^{3D}(\xi^1,\xi^2,\xi^3) = \underline{u}(\xi^1,\xi^2) + \xi^3 \theta_\lambda(\xi^1,\xi^2)\underline{a}^\lambda(\xi^1,\xi^2). \tag{9}$$

The first term $\underline{u}$ represents the global infinitesimal displacement of a line perpendicular to the midsurface at the coordinates (ξ^1,ξ^2). The second term is the displacement due to the rotation of this line.

The deformation of the membrane is computed from the displacement. The expression of the nonlinear 3D Green-Lagrange strain tensor is

$$e_{ij} = \frac{1}{2}\left(\underline{g}_i \cdot \underline{u}^{3D}_{,j} + \underline{g}_j \cdot \underline{u}^{3D}_{,i} + \underline{u}^{3D}_{,i} \cdot \underline{u}^{3D}_{,j} \right) \qquad i,j = 1,2,3. \tag{10}$$

The second Piola-Kirchhoff tension tensor $\underline{\underline{\Sigma}}$ is then obtained from

$$\underline{\underline{\Sigma}} = \frac{\partial w(\underline{u}^{3D})}{\partial \underline{\underline{e}}}, \tag{11}$$

where the strain energy function takes the form

$$w(\underline{u}^{3D}) = \frac{1}{2}\int_{\omega^{3D}} \left[C^{\alpha\beta\lambda\mu} e_{\alpha\beta}(\underline{u}^{3D}) e_{\lambda\mu}(\underline{u}^{3D}) + D^{\alpha\lambda} e_{\alpha 3}(\underline{u}^{3D}) e_{\lambda 3}(\underline{u}^{3D}) \right] d\omega \qquad \alpha,\beta,\lambda,\mu = 1,2. \tag{12}$$

with

$$C^{\alpha\beta\lambda\mu} = G_s \left(g^{\alpha\lambda} g^{\beta\mu} + g^{\alpha\mu} g^{\beta\lambda} + \frac{2\nu_s}{1-\nu_s} g^{\alpha\beta} g^{\lambda\mu} \right), \tag{13}$$

$$D^{\alpha\lambda} = 4 G_s g^{\alpha\lambda} \tag{14}$$

for the Hooke's law. Tensions, which are forces per unit length of the deformed midsurface, are obtained integrating the stresses across the wall thickness.

Knowing the internal tension tensor, the unknown viscous load exerted by the fluid on the membrane can be calculated solving the wall equilibrium

$$\nabla_s \cdot \underline{\underline{T}} + \underline{q} = \underline{0}. \tag{15}$$

The operator ∇_s is the surface gradient and $\underline{\underline{T}}$ the Cauchy tension tensor such that

$$\underline{\underline{T}} = \frac{1}{J}\, \underline{\underline{F}} \cdot \underline{\underline{\Sigma}} \cdot \underline{\underline{F}}^T \tag{16}$$

with J the Jacobian and $\underline{\underline{F}}$ the deformation gradient with respect to the reference configuration.

The local equilibrium (15) is then written in a weak form using the virtual work principle and solved by means of the finite element method. Let $\mathcal{V}$ be the Sobolev space H^1. For any virtual displacement field $\underline{\hat{u}}^{3D} \in \mathcal{V}$, the internal and external virtual work balance requires

$$\int_{\omega^{3D}} \underline{\hat{u}}^{3D} \cdot \underline{q}\, d\omega = \int_{\omega^{3D}} \underline{\underline{\Sigma}} : \underline{\underline{\delta\hat{e}}}\, d\omega \tag{17}$$

where $\underline{\underline{\delta\hat{e}}} = \underline{\underline{e}}(\underline{U}^{3D} + \underline{\hat{u}}^{3D}) - \underline{\underline{e}}(\underline{U}^{3D})$ with $\underline{U}^{3D}$ the displacement in the reference configuration. The equation is solved to compute the load $\underline{q}$.

2.1.1 Internal and external flow dynamics

Since the Reynolds numbers are infinitely small, the flows are governed by the Stokes equations. Knowing the load $\underline{q}$, the velocity of the points can be expressed as an integral equation over the deformed capsule surface $\mathcal{S}$ using the boundary integral method :

$$\forall \underline{\phi}_0^{3D} \in \omega^{3D}, \quad \underline{v}(\underline{\phi}_0^{3D} = \underline{v}^{\infty}(\underline{\phi}_0^{3D})) - \frac{1}{8\pi\mu} \int_S \left(\frac{\mathbb{I}}{\| \underline{r} \|} + \frac{\underline{r} \otimes \underline{r}}{\| \underline{r} \|^3} \right) \cdot \underline{q}(\underline{\phi}^{'3D}) dS(\underline{\phi}^{'3D}), \tag{18}$$

where $\underline{v}^{\infty}$ is the undisturbed flow velocity and $\mathbb{I}$ is the identity vector. The vector $\underline{r} = \underline{\phi}^{3D} - \underline{\phi}^{'3D}$ is the distance vector between the point $\underline{\phi}^{3D}$, where the velocity vector is calculated, and the point $\underline{\phi}^{'3D}$ that describes the midsurface $\mathcal{S}$ in the integral.

The displacement is related to the velocity $\underline{v}$ of the wall through the kinematic condition :

$$\underline{v}(\xi^1, \xi^2, \xi^3) = \underline{u}^{3D}_{,t}(\xi^1, \xi^2, \xi^3) \tag{19}$$

where $\cdot_{,t}$ is the time derivative. An explicit Euler method is then used to integrate the velocity over time and obtain the new position of the wall points.

2.2 Discretization

The capsule wall is discretized using triangular linear shell finite elements. We use the mixed interpolation of the tensorial component approach, which can handle the modeling of objects with wall thicknesses much smaller than their characteristic size, a situation that is prone to locking phenomena [2, 5, 8]. The MITC approach is based on a mixed formulation that interpolates strains and displacements separately and connects both interpolations at specific tying points. In the following, we will show results for MITC3 linear elements consisting of three nodes (one at each vertex) with 5 degrees of freedom by node.

The mesh of the spherical capsule is generated by inscribing an icosahedron (regular polyhedron with 20 triangular faces) in a sphere. The elements are subdivided sequentially until the desired number of elements is reached [7, 9]. We denote h the mesh size.

3 Inflation of a capsule under an internal pressure

Before coupling the finite element method to the fluid solver, we have validated the mechanical behavior of the shell finite elements in large static deformations. We consider a spherical capsule inflated from radius ℓ to radius $\ell_p = (1+\alpha)\ell$ by an internal pressure p [9]. During the inflation, the wall is subjected to an isotropic traction characterized by the stretch ratio $\lambda = 1+\alpha$. Numerically, it is simulated by imposing a normal displacement. The bending resistance plays no role in this test case . We are thus supposed to find the same results as those obtained when the capsule wall is modeled as a membrane devoid of bending stiffness

When the capsule wall is modeled as a 2D isotropic material obeying the generalized Hooke's law [1], the isotropic principal tensions T is related to λ by

$$T = G_s(\lambda^2 - 1)\frac{1+\nu_s}{1-\nu_s}. \tag{20}$$

We thus have an exact analytical relation between the pressure and the inflation ratio α. In our case, we have chosen $\nu_s = 0.5$ to account for the material incompressibility.

The analytical expression of the pressure is deduced from the Laplace's law

$$p = \frac{2T}{\ell_p} = \frac{2T}{(1+\alpha)\ell}. \tag{21}$$

Figure 1 shows the non-dimensional pressure $p\ell/G_s$ obtained numerically as a function of the inflation factor α for several bending numbers B, when the capsule is modeled with MITC3. The relative error ε relative to the analytical value $(p\ell/G_s)_{ana}$ is defined by

$$\varepsilon = \frac{|(p\ell/G_s)_{ana} - (p\ell/G_s)|}{(p\ell/G_s)_{ana}}. \tag{22}$$

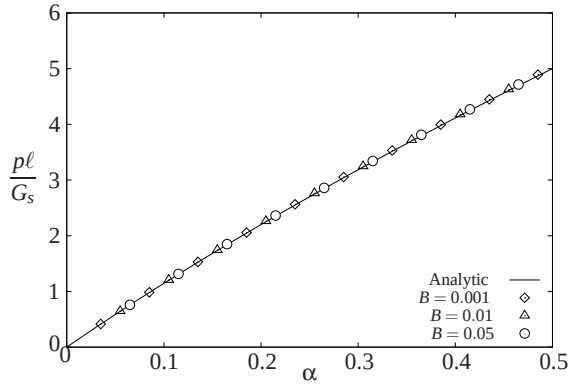

Fig. 1 – Non-dimensional pressure as a function of the inflation factor α for bending numbers $B = 0.01, 0.05$ and 0.1 of a capsule wall discretized with 1280 MITC3 elements.

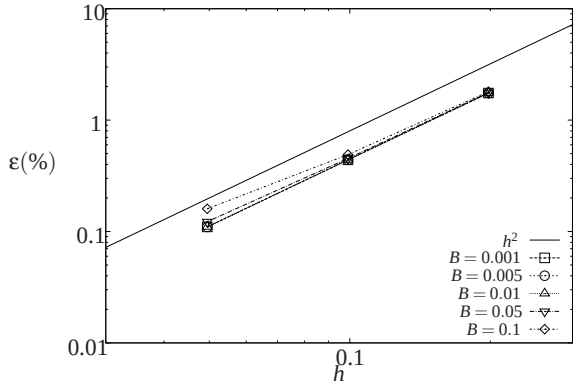

Fig. 2 – Relative error ε as a function of the mesh size h for bending numbers $B = 0.001, 0.005, 0.01, 0.05$ and 0.1 of a capsule wall discretized with 1280 MITC3 elements.

The error remains small in all cases. It increases with increasing wall thickness η and decreasing number of elements. Among the simulated cases, it is therefore maximum when the capsule is modeled with $B = 0.1$ and 1280 MITC3 elements. Even in this case, it is only equal to 0.49%, which validates the shell finite element method. In the following, all the results are provided for 5120 elements. The characteristic mesh size is then $h = 5 \times 10^{-2}$.

The convergence of the finite element solver with the mesh size is provided in figure 2. The relative error is plotted as a function of the mesh size for various bending numbers B. We notice that the numerical procedure converges as h^2 regardless the bending number.

4 Capsule dynamics in a simple shear flow

4.1 Convergence

We now consider the dynamics of an initially spherical capsule in a simple shear flow at $Ca = 0.6$. At steady state the capsule assumes a quasi-ellipsoidal shape and is elongated in the straining direction. The deformed shape can be approximated by its ellipsoid of inertia. We define L_1 and L_2 the lengths of the two principal axes of the ellipsoid of inertia in the shear plane. The deformation of the capsule in the shear plane can then measured by the Taylor parameter D_{12} :

$$D_{12} = \frac{L_1 - L_2}{L_1 + L_2}. \tag{23}$$

We call D_{12}^{∞} the value of the Taylor parameter D_{12} at steady state.

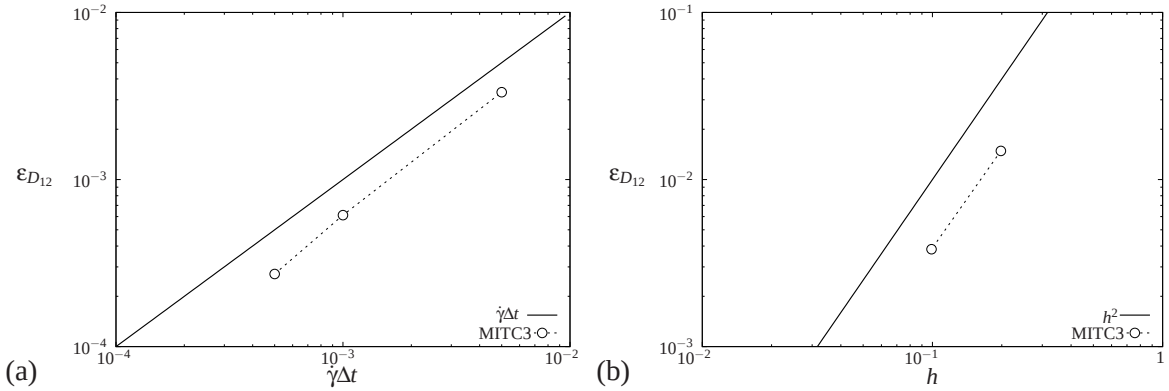

Fig. 3 – Capsule at $Ca = 0.6$: relative error $\varepsilon_{D_{12}}$ on the Taylor parameter D_{12}^{∞} as a function of (a) the time step and (b) the mesh size. (a) The capsule is meshed with 5120 MITC3 elements ($h = 5 \times 10^{-2}$). The reference value D_{12}^{ref} corresponds to $\dot{\gamma}\Delta t = 1 \times 10^{-4}$. (b) The time step is $\dot{\gamma}\Delta t = 1 \times 10^{-4}$. The reference value D_{12}^{ref} corresponds to 5120 MITC3 elements.

We first study the convergence with the dimensionless time step $\dot{\gamma}\Delta t$. Since no analytical solution of the fluid-structure interaction problem exists, we choose as reference value the value of D_{12}^{∞} obtained when $\dot{\gamma}\Delta t = 1 \times 10^{-4}$. This value is denoted D_{12}^{ref}. We compute the relative error $\varepsilon_{D_{12}} = |D_{12}^{\infty} - D_{12}^{ref}|/D_{12}^{ref}$. According to figure 3 (a), the numerical procedure converges linearly with Δt. It is important to note that the relative error remains small ($\varepsilon_{D_{12}} < 3 \times 10^{-3}$) for all the time steps considered.

We then analyze the influence of the mesh size. As shown in figure 3 (b), the coupled numerical procedure converges quadritically with h. However, at time of writing, we are not able to get more than 5120 elements and consequently we cannot have $h < 0.1982$.

4.2 Influence of the bending resistance on the capsule dynamics

For all the values of the bending number ($B \neq 0$), the capsule is elongated in the straining direction at the steady state, while the vorticity of the flow induces the rotation of the wall around the steady deformed shape. The larger the capillary number, the more elongated the capsule (figure 4). This motion, called *tank-treading*, is exactly the same as that observed when the wall of the capsule is modeled with a membrane model ($B = 0$) [7, 4, 9].

To determine the influence of the bending resistance on the average shape in the shear plane, we compare the Taylor parameter at steady state D_{12}^{∞} for several capillary numbers and two values of bending number B (Figure 5). For a given capillary number, the capsule has the same average shape in the shear plane as the one predicted when the capsule wall is modeled as a two-dimensional membrane (without bending resistance).

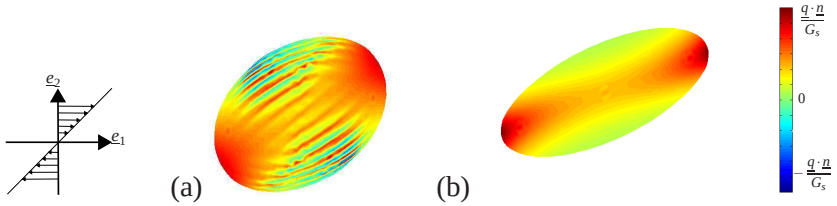

Fig. 4 – Steady deformed shape for a capsule with $B = 0.005$ at (a) $Ca = 0.1$ and (b) $Ca = 0.6$. The color scale corresponds to the normal load $\underline{q}\cdot\underline{n}$, where the maximum value is equal to $\underline{q}\cdot\underline{n}/G_s = 0.5$ at $Ca = 0.1$ and 2.5 at $Ca = 0.6$.

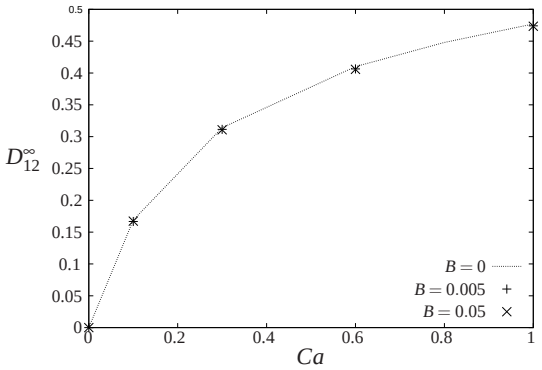

Fig. 5 – Values of D_{12}^{∞} as a function of Ca for bending numbers $B = 0, 0.005$ and 0.05, for an initially spherical capsule subjected to a simple shear flow.

When the capsule wall is modeled with a membrane model ($B = 0$), wrinkles appear in the central region of the capsule for capillary numbers below a critical value Ca_L (Figure 6a). They result from the presence of compressive tensions in the equatorial area and are in the straining direction. They persist at steady state. Wrinkles are observed at exactly the same location with the shell model (Figure 6 b,c) for low values of B. When the bending number is increased, the wrinkle wavelength decreases : it is due to the increase in bending stiffness (Figure 6 b,c). For $B = 0.05$, the wrinkles no longer form (Figure 6 d). There is therefore a critical bending number, above which the capsule wall is too stiff for buckling to occur.

For capillary numbers above Ca_L, the capsule is more elongated by the flow (Figure 4b) : the tensions at the equator become positive and the wrinkles disappear.

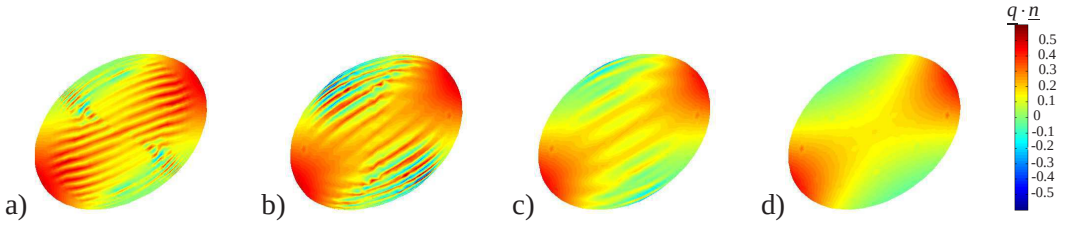

Fig. 6 – Steady-state profiles of capsules subjected to a simple shear flow (Ca=0.1) : bending number $B = 0$ (membrane model) (a), $B = 0.005$ (b), $B = 0.01$(c) and $B = 0.05$ (d).

5 Conclusion

We have simulated the motion of a capsule in a simple shear flow using a boundary integral - MITC shell finite element coupling strategy. The numerical method is stable and free of locking phenomenon. We have shown that the motion and deformation of a thin membrane capsule is marginally influenced by the bending stiffness. The latter controls the amplitude and wavelength of the wrinkles that appear at low capillary number in the straining direction. However, the average deformed shape that the capsule assumes, as it tank-treads, remains identical to that predicted by a two-dimensional membrane model.

Références

[1] D. Barthès-Biesel, A. Diaz, E. Denin *Effect of constitutive laws for two-dimensional membranes on flow-induced capsule deformation.* J. Fluid Mech., 460, 211-222, 2002.

[2] D. Chapelle, K. J. Bathe *The Finite Element Analysis of Shells - Fundamentals.* Computation Fluid and Solid Mechanics. Springer.

[3] C. Dupont, A.-V. Salsac, D. Barthès-Biesel *Off plane motion of a prolate capsule in shear flow.* J. Fluid Mech., In press.

[4] É. Lac, D. Barthès-Biesel, N. A. Pelekasis, J. Tsamopoulos. *Spherical capsules in three-dimensional unbounded Stokes flow : effect of the membrane constitutive law and onset of buckling.* J. Fluid Mech., 516, 303–334, 2004.

[5] P.-S. Lee, K.-J. Bathe. *Development of MITC isotropic triangular shell finite elements.* Comp. Struct, 82, 945–962, 2004.

[6] C. Pozrikidis. *Finite deformation of liquid capsules enclosed by elastic membranes in simple shear flow.* J. Fluid Mech., 297, 123–152, 1995.

[7] S. Ramanujan, C. Pozrikidis. *Deformation of liquid capsules enclosed by elastic membranes in simple shear flow : Large deformations and the effect of capsule viscosity.* J. Fluid Mech., 361, 117–143, 1998.

[8] I. Paris Suarez *Robustesse des éléments finis triangulaires de coque.* phD Thesis, Université Pierre et Marie Curie (Paris VI), 2006.

[9] J. Walter, A.-V. Salsac, D. Barthès-Biesel, P. Le Tallec. *Coupling of finite element and boundary integral methods for a capsule in a Stokes flow.* Int. J. Num. Meth. Engng, 83, 829–850, 2010.

[10] X.-Q. Hu, A.-V. Salsac, D. Barthès-Biesel *Fow of a spherical capsule in a pore with circular or square cross-section.* J. Fluid Mech., 705, 176–194, 2012.